Reply to "Comment on 'From Nanoparticles to Nanoplates: Preferential Oriented Connection of Ag Colloids during Electrophoretic Deposition'"

ARTICLE *in* THE JOURNAL OF PHYSICAL CHEMISTRY C · APRIL 2009

Impact Factor: 4.77 · DOI: 10.1021/jp901961h

From Nanoparticles to Nanoplates: Preferential Oriented Connection of Ag Colloids during Electrophoretic Deposition

Shikuan Yang, Weiping Cai,* Guangqiang Liu, and Haibo Zeng

Key Laboratory of Materials Physics, Anhui Key Laboratory of Nanomaterials and Nanotechnology, Institute of Solid State Physics, Chinese Academy of Sciences, Hefei 230031, People's Republic of China

Received: March 3, 2009; Revised Manuscript Received: March 29, 2009

The Ag nanostructured films are fabricated based on electrophoretic deposition (EPD) in the Ag colloidal solution produced by laser ablation in water, under a constant current deposition mode. It has been found that the obtained films are of tunable and controllable morphologies and structures depending on EPD parameters. Importantly, there exists significant crystal growth for the building blocks of the film during EPD, in addition to normal particles' coagulation. With increasing the current density of EPD, the size of the building blocks in the film decreases, and the shape evolves from polyhedral particles to regular nanoplates, and to irregular equi-axial particles. Correspondingly, the film structure changes from discontinuous film, consisting of the isolated aggregates of the building blocks, to the homogeneous and dense film, consisting of equi-axial particles. Further experiments have revealed that formation of the regularly shaped single crystal building blocks is attributed to the crystal growth induced by the oriented connection of the nanoparticles, with fresh surface, in the colloidal solution and/or on the substrate during EPD. This study not only provides a new method to control and tune the morphology and structure of films in a simple way, but also deepens the understanding of the physical mechanism of EPD.

1. Introduction

Electrophoretic deposition (EPD) as a material processing technique has attracted much attention due to its low cost, versatile property, and simple equipment.[1−16] It is usually carried out in a two-electrode cell with colloidal solution, as schematically shown in Scheme 1. There are mainly two steps. First, charged colloidal particles suspended in a suitable solution move toward the oppositely charged electrodes under an applied electric field; second, the colloidal particles accumulate on the electrode and produce a compact and homogeneous film.[1−12] This method was initially used for processing traditional ceramics and depositing various coatings (such as TiO_2, ZnO, SiC, etc.) on substrates with various shapes or porous structures.[1−9] Furthermore, assisted with templates, TiO_2 nanowire arrays have also been acquired.[13] However, EPD is seldom used for fabrication of noble metal film structures,[14−16]which are well-known for their surface enhanced Raman scattering (SERS) properties. Particles (or building blocks) in the film prepared by EPD are usually similar in size and shape to those in the initial colloidal solution.[1−16] This means that it is difficult to tune and control the morphology and structure of the films by EPD without templates, and no report on the EPD-induced crystal growth has been found, to the best of our knowledge. It is important to control the film's morphology and structure for some properties, such as SERS for a noble metal film.[17]

Recently, we have produced films with tunable and controllable morphologies and structures, based on EPD in the Ag colloidal solution, produced by laser ablation (LA) of a Ag flake in deionized water, under a constant current deposition mode. It has been found that there exists significant crystal growth during EPD, in addition to normal particles' coagulation. With increasing the current density of EPD, the shape of the building blocks in the film evolves from polyhedral particles to regular nanoplates, and to irregular equi-axial particles. Further experiments have revealed that formation of the regularly shaped single crystal building blocks is attributed to the crystal growth, induced by oriented connection of the nanoparticles (NPs) in the colloidal solution and/or on the substrate during EPD. In addition, the Ag colloidal solution prepared by LA in deionized water is also crucial to such crystal growth during EPD. However, the Ag colloidal solution prepared by some other methods cannot lead to such crystal growth during EPD. This study not only provides a new method to control and tune the morphology and structure of films in a simple way, but also deepens the understanding of the physical mechanism of EPD.

SCHEME 1: Schemic Illustration of Electrophoretic Deposition in a Colloidal Solution

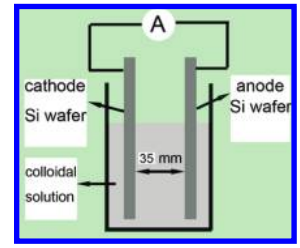

2. Experimental Section

2.1. Preparation of Ag Colloid. The Ag colloidal solution was first prepared by laser ablation of a Ag flake (>99.9%) immersed in deionized water, as previously described.[18] Briefly, The Ag flake was supersonically rinsed in deionized water and then ethanol for 1 h, respectively. The cleaned Ag flake was immersed in a vessel filled with 8 mL of deionized water. The flake was irradiated by the first harmonic (1064 nm) Nd:YAG

* To whom correspondence should be addressed. E-mail: wpcai@issp.ac.cn. Fax: +86-551-5591434.

10.1021/jp901961h CCC: $40.75
Published on Web 04/14/2009

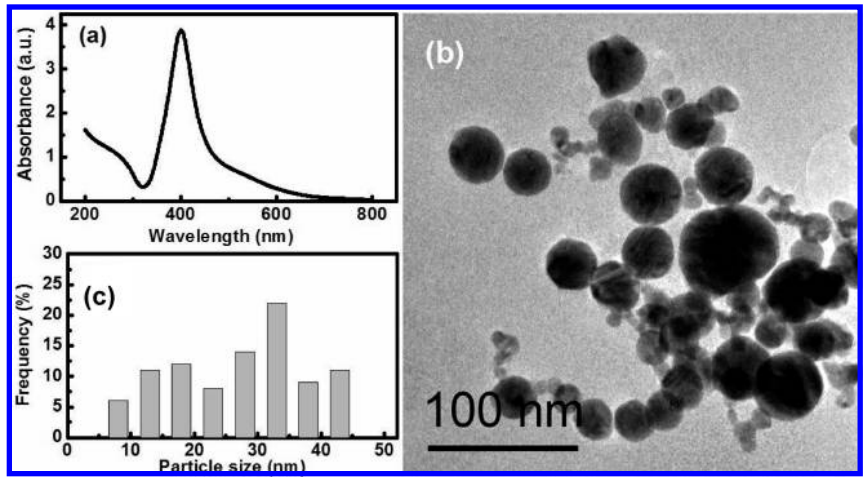

Figure 1. Optical absorption spectrum (a), the corresponding TEM image (b), and the particles' size distribution (c) for the freshly prepared colloidal solution by laser ablation.

laser, operated at 100 mJ/pulse with a pulse duration of 10 ns and a frequency of 10 Hz. The laser beam was focused with a spot size about 2 mm in diameter by using a lens with a focal length of 150 mm. The solution was continuously stirred during irradiation. After irradiation for 30 min, a yellowish Ag colloidal solution was obtained. The Ag content in the solution can be estimated to be about 0.05 g/L by the mass loss of the Ag flake.

2.2. Electrophoretic Deposition. EPD was carried out at a constant current density of 50 μA/cm^2 for 14 h, as schematically illustrated in Scheme 1. Two cleaned Si wafers were used as cathode and anode electrodes both with a working area of 1 cm $\times$ 1.5 cm, immersed into the as-prepared Ag colloidal solution (about 16 mL). The distance between the two electrodes was maintained at 35 mm. After electrophoresis, the deposited samples were rinsed softly by deionized water and then dried by nitrogen flow.

2.3. Characteration. Morphology of the samples was examined by a field-emission scan electron microscope (FESEM). X-ray diffraction (XRD) was measured on an X-ray diffractometer (the Philips X'Pert) with Cu Kα line (0.15419 nm). Transmission electron microscopic (TEM) examination was conducted on a JEM-200CX operated at 200 kV. The optical absorption spectra were measured on a Cary-5E UV−vis−NIR spectrophotometer. ζ potential was measured by using a Zetasizer 3000 (England, MALVERN).

3. Results and Discussion

The as-prepared colloidal solution is stable without precipitation at least for one month. ζ potential measurement demonstrates that the Ag NPs in the solution (pH 7) are charged. Its optical absorption spectrum shows a peak located around 400 nm, as shown in Figure 1a, which is the well-known surface plasmon resonance of Ag NPs.[19] TEM observation has indicated nearly spherical nanoparticles with about 30 nm in mean size in the colloidal solution (Figure 1, panels b and c). The corresponding selected area diffraction pattern (SAED) has confirmed that the NPs are Ag with face-centered-cubic (fcc) structure. As for the formation of the NPs during LA in liquid, there are many reports.[18,20−23] In our case, Ag plasma will be formed on the interface between the Ag flake and deionized water instantly after interaction of the pulsed laser with the Ag flake. Subsequently, such Ag plasma ultrasonically and adiabatically expands, leading to cooling of the Ag plume region and hence to formation of Ag clusters. With extinguishment of the plasma, such formed clusters aggregate quickly into Ag NPs.

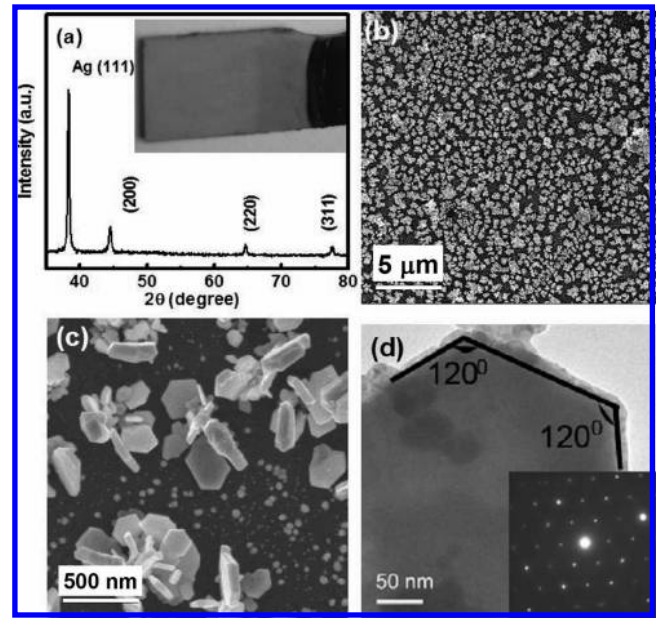

Figure 2. Structure and morphology of the sample prepared by electrophoretic deposition under 50 μA/cm^2 for 14 h on Si wafer. (a) XRD result. Inset: A photo of the sample. (b, c) FESEM images with different magnifications. (d) TEM image of a single nanoplate. Inset: The corresponding SAED pattern.

3.1. Morphology and Microstructure. After EPD under the current density of 50 μA/cm^2 for 14 h in the colloidal solution, a homogeneous film on Si (cathode) was obtained (see the photo in the inset of Figure 2a). XRD shows the obtained film is Ag with fcc structure, as shown in Figure 2a. Further, FESEM observation indicates that the film consists of many isolated aggregates (see Figure 2b). The local magnification has revealed that the aggregates are composed of polygonal or regular Ag nanoplates with about 160 nm in edge length and 60 nm in thickness (or 200−400 nm in planar dimension of the plates), as clearly seen in Figure 2c, in contrast to the morphology of laser-ablated Ag NPs shown in Figure 1b, and among the isolated aggregates, there exist some Ag NPs less than 50 nm in size (similar to those in the original colloidal solution). TEM examination, by scalping the film and dispersion in ethanol, shows that the angle between the adjacent edges for the many nanoplates is about 60° or 120°, as seen in Figure 2d. The SAED, by aligning the electron beam perpendicular to the planar surface of the nanoplate, has revealed that the planar surface of

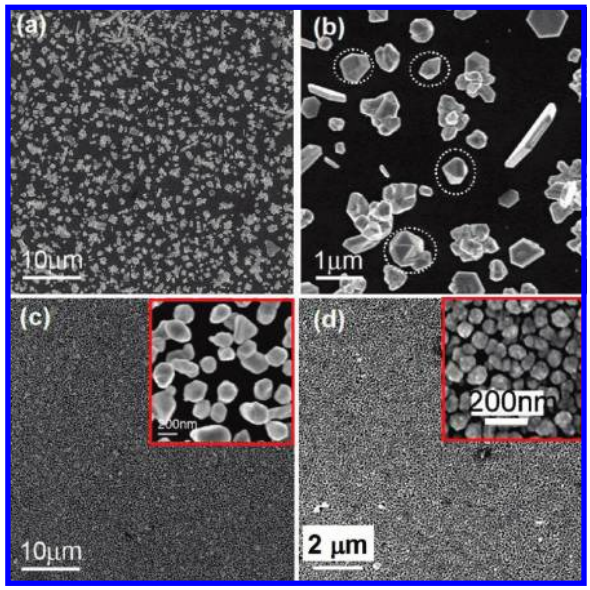

Figure 3. Influence of the deposition current on the Ag film morphology: panels a and b correspond to 20 μA/cm^2 for 14 h with different magnifications; panels c and d correspond to 80 and 100 μA/cm^2 for 14 h, respectively. Insets: The corresponding local magnification.

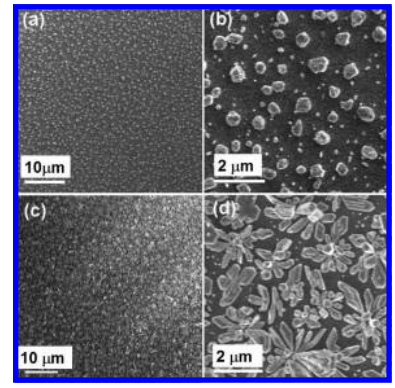

Figure 4. The FESEM images of the Ag films after EPD on ITO glass for 14 h under different current densities: (a, b) 20 μA/cm^2 with different magnifications; (c, d) 50 μA/cm^2 with different magnifications.

the plate is parallel to {111}. The hexagonal symmetry of the diffraction spots indicates that the plate is a single crystal. These results imply that the crystal growth occurs on the substrate and/or in the colloidal solution during EPD.

3.2. Influence Factors. Further experiments have shown that formation of the Ag nanoplates during EPD depends on the current density and species of the substrates.

3.2.1. Current Density. Figure 3 shows the morphological evolution of the films with the current density during EPD. An increase of the current density leads to the morphological change and size reduction of the particles on the substrate. When the current density is low (lower than 50 μA/cm^2, say, 20 μA/cm^2), the formed film is composed of the isolated aggregates, as illustrated in Figure 3a, similar to that shown in Figure 2b. However, the local magnification exhibits that the aggregates consist of particles with polyhedral shape and about 500 nm in size (see the circular marks in Figure 3b). There are only a few nanoplates observed and some of them are of hexagonal or truncated triangular shape of about 400 nm in edge length and 100 nm in thickness, as shown in Figure 3a,b. High current density (> 50 μA/cm^2, say, 80 μA/cm^2) will induce nearly equiaxial particles of about 170 nm in size, dispersed on the substrate homogeneously (Figure 3c and inset). The higher current density (say, 100 μA/cm^2) results in the homogeneous but denser film consisting of the smaller particle of only about 85 nm in size (Figure 3d and inset). Only the appropriate deposition current (or about 50 μA/cm^2) leads to the formation of the Ag nanoplates on the substrate (Figure 2c,d). We can thus control or tune the structure and morphology of the film by EPD.

3.2.2. Substrate. If we use indium tin oxide (ITO) glass instead of an Si wafer as electrodes, the morphology of the final film is different. Low current (20 μA/cm^2) results in the formation of particles with two types of size distribution on the substrate. The large particles are about 500 nm in mean size and the small ones are around 100 nm (Figure 4a,b). The current at 50 μA/cm^2 leads to the film consisting of many thick slats of about 1 μm in length and 0.5 μm in width (Figure 4c,d). These results indicate that crystal growth also occurs on the substrate during EPD. Otherwise, the morphology of the building blocks in the film should be independent of substrate.

3.3. Crystal Growth During EPD. The Ag NPs in colloidal solution are stabilized electrostatically against agglomeration. Such electrostatic stabilization is based on surface charge of the NPs, which will interact with the other charged species in the solution to form an electric double-layer structure capping the NPs and prevent the NPs from approaching each other.[13] Upon applying an external electric field, the EPD process occurs. According to Derjaguin−Landau−Verwey−Overbeek (DLVO) theory,[6] the charged NPs in the colloidal solution are in motion in response to the electric field. Some moving colloids will join together due to the collision induced by the difference in motion velocity of the particles with different sizes, leading to distortion of the electric double layer, as discussed by Sarkar and Nicholson,[6,9] and to coagulation of the collided NPs. Finally the initial nanoparticles and coagulated particles move toward and deposit on the anodic or cathodic electrode (depending on the charge property of the NPs), forming a homogeneous film in which the building blocks are usually similar in size and shape to NPs in the initial colloidal solution. Some too large coagulated particles sink before moving onto the substrate. Obviously, the crystal growth of the particles is usually negligible during EPD, as previously extensively reported.[1−16]

In our case, however, the situation is different. The significant crystal growth of the particles takes place in the solution and/or on the substrate under appropriate electrophoretic conditions. This can be attributed to the oriented connection of Ag NPs in the colloidal solution, prepared by LA in deionized water, during EPD.

3.3.1. Oriented Connection of Ag NPs. It is known that there exists an interface between two randomly conjoined single crystal particles. Thermodynamically, these two conjoined particles will rotate or fine-tune to become the same orientation so that the interface disappears and the free energy decreases, i.e., the two conjoined single crystal particles will merge into one larger single crystal particle, what we call oriented connection growth.[24−29] In principle, if only the NPs (single crystal) in the solution are active enough and the time is sufficiently long, such oriented connection growth should take place.

In this study, since the Ag colloidal solution was prepared by LA in deionized water, Ag NPs were formed in the water without exposure to air or some additives and retain the fresh surfaces, in contrast to the products prepared by the conventional methods which lead to surface adsorption or passivation. Obviously, the NPs with fresh surfaces should conjoin, after collision, more easily in the solution during EPD (see step I in

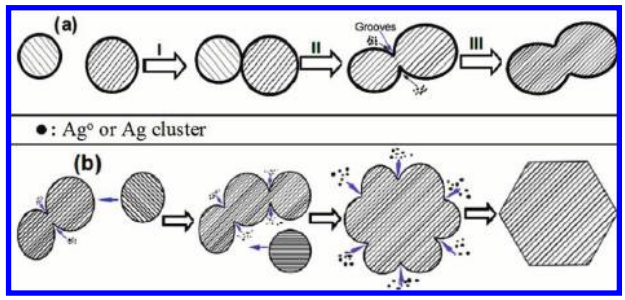

Figure 5. Schematic illustration of crystal growth during EPD: (a) Oriented connection growth—(I) collision of two NPs, (II) self-orientation modulation and merging into a single particle, and (III) preferential attachment of Ag atoms and/or clusters on the grooves and gradual disappearance of the grooves; (b) formation of a Ag nanoplate by preferentially oriented connection growth and attachment of Ag atoms and/or clusters on the groove.

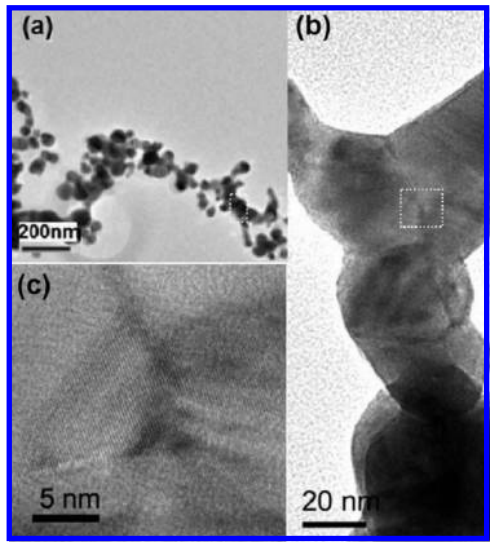

Figure 6. TEM image of the Ag aggregates (a) sinking on the bottom of the bath from the electrophoretic colloidal solution. (b) Magnification of the frame marked in panel a. (c) HRTEM image for the area marked in panel b.

Figure 5a). The conjoined NPs will be self-modulated to the same orientation, merging into one larger particle with enough time (see step II in Figure 5a). Such oriented connection growth has been confirmed, as demonstrated in Figure 6, corresponding to the conjoined nanoparticles which sink in the solution during EPD. The particles on both sides of the groove are of the same orientation (see Figure 6c). The grooves should originate from the link between the initial nanoparticles. Also, there inevitably exist reduced Ag° atoms or Ag clusters in the as-prepared colloidal solution due to the laser ablation of Ag target in water. Thus, such grooves will disappear after enough time, due to preferential attachment of the Ag° atoms or clusters on them (see step III in Figure 5a).

From the viewpoint above, such oriented connection growth would be difficult for the NPs without a fresh surface (or with molecular adsorption). For further confirmation, EPD was conducted in the Ag colloidal solution prepared by LA in sodium dodecyl sulfate (SDS) aqueous solution (0.05 M). The final film consists of particle-aggregates, and no oriented connection growth was observed, as shown in Figure 7a,b. Similarly, if EPD is carried out in the Ag colloidal solution prepared by a normal chemical route,[30] no oriented connection growth occurs, as illustrated in Figure 7c. For both colloidal solutions, Ag NPs

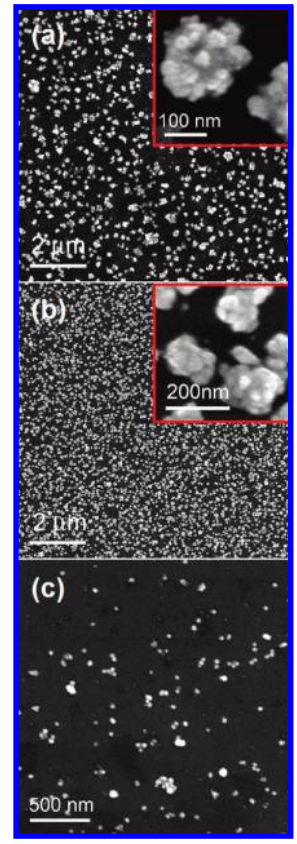

Figure 7. FESEM images of the Ag films on Si wafers after EPD for 14 h in the Ag colloidal solutions prepared by different methods. Panels a and b correspond to the EPD in the Ag colloidal solution prepared by LA in SDS aqueous solution under 50 and 100 μA/cm^2, respectively. Insets: The local maginification. Panel c corresponds to the EPD in the Ag colloidal solution prepared by a normal chemical route[30] under 50 μA/cm^2.

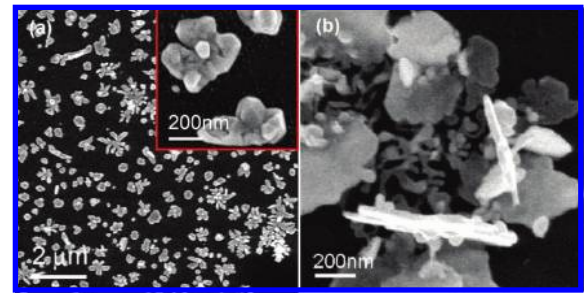

Figure 8. FESEM images of Ag films after EPD under 50 μA/cm^2 for different times: (a) 2 (inset: a local magnification) and (b) 9 h.

possess no fresh surface due to the inevitable existence of additives' adsorption on the colloidal surface.

3.3.2. Formation of Ag Nanoplates. From the viewpoint of energy, the link between two crystals takes place more easily on the surface with high free energy than on that with low energy such as {111} for Ag. This means that the preferentially oriented connection will occur under the appropriate deposition conditions. Here when the current of EPD is about 50 μA/cm^2, the connection growth takes place preferentially along {111} after collision and self-modulation of the NPs in the solution, as schematically illustrated in Figure 5b, leading to formation of Ag nanoplates with rough surface morphology. Figure 8 shows the morphological evolution of the nanoplates, induced by oriented connection of Ag NPs, during EPD. EPD for 2 h leads to many island-like objects, with 200−300 nm dimension and several grooves due to the oriented connection of NPs,

formed on the substrate (see the inset in Figure 8a). Obviously, during EPD, preferential attachment of Ag° atoms or Ag clusters in the solution will also take place on the grooves of the island-like nano-objects, which will lead to formation of the planar morphology after enough time. Figure 8b has confirmed that such nano-objects have evolved to plate-like shape after deposition for 9 h. In the SEM fields, there are only a very few plates with regular shape observed after EPD for 9 h. Only after deposition for enough time are the regular nanoplates formed by preferential attachment of Ag° atoms or Ag clusters in the solution on the grooves of the nano-objects (Figure 2b−d or Figure 5b).

Obviously, when the current density is high, corresponding to high deposition potential, the Ag NPs move fast in the solution. Because there is not enough time to finish orientation modulation, the NPs will coagulate after collision in the solution and form equi-axial big particles (Figure 3 c,d) instead of nanoplates. Furthermore, after the initial NPs or coagulated particles deposit on the substrate, orientation modulation and Ag° atoms (or clusters) attachment will still take place during EPD under relatively low current density (50 μA/cm^2 or lower), which leads to different morphology on the Si wafer and ITO glass due to their different effects on the orientation modulation (see Figures 2b,c and 4c,d).

As for the size dependence of the building blocks in the films on deposition current, it is easily understood. The high deposition current density (or high deposition potential) corresponds to the high migration speed of NPs in the solution. The coagulated particles have only a short migration time in the solution before deposition on the substrate, and thus the final size should be small. Otherwise, the building blocks in the films will be big in size since there is a long time in the solution for the oriented connection growth or coagulation.

4. Conclusions

In summary, we fabricate the Ag nanostructured films using electrophoretic deposition (EPD) in the Ag colloidal solution produced by laser ablation of a Ag flake in water, under a constant current deposition mode. The morphologies and structures of the obtained films are tunable and controllable depending on EPD parameters, especially the current density of EPD. With increasing the current density, the building blocks in the film evolve from polyhedral particles to regular nanoplates, and to irregular equi-axial particles. Correspondingly, the film structure changes from discontinuous film, consisting of the isolated aggregates of the building blocks, to the homogeneous and dense film, consisting of equi-axial particles. The size of the building blocks in the film decreases with increasing the current density, due to ever-reducing migration time of the particles in the solution before deposition on substrate. Importantly, there exists significant crystal growth during EPD leading to the regularly shaped building blocks in the film. This is attributed to the (preferentially) oriented connection of the nanoparticles, with a fresh surface (without additives' adsorption) in the colloidal solution and/or on the substrate at a long enough time during EPD. This study provides a new method to control and tune the morphology and structure of films in a simple way, and deepens the understanding of the physical mechanism of EPD.

Acknowledgment. This work is financially supported by the Natural Science Foundation of China (Grant Nos. 50671100 and 50831005), the Major State research program of China "Fundamental Investigation on Micro-Nano Sensors and Systems based on BNI Fusion" (Grant No. 2006CB300402), and the Knowledge Innovation Program of the Chinese Academy of Sciences (Grant No. KJCX2-SW-W31).

References and Notes

(1) Ferrari, B.; Castro, Y.; Gallardo, J.; Moreno, R.; Duran, A. Spanish Patent P 200 008, 525, 2000.
(2) Formento, A.; Montanaro, L. *J. Am. Ceram. Soc.* **1999**, *82*, 3521.
(3) Sarkar, P.; Haung, X.; Nicholson, P. S. *J. Am. Ceram. Soc.* **1992**, *75*, 29070.
(4) Pickard, W. F. *J. Electrochem. Soc.* **1968**, *115*, 105C.
(5) Vleugels, J.; Xu, T.; Huang, S.; Kan, Y.; Wang, P.; Li, L.; Van der Biest, O. O. *J. Eur. Ceram. Soc.* **2007**, *27*, 1339.
(6) Sarkar, P.; Nicholson, P. S. *J. Am. Ceram. Soc.* **1996**, *79*, 1987.
(7) Boccaccini, A. R.; Zhitomirsky, L. *Curr. Opin. Solid State Mater. Sci.* **2002**, *6*, 251.
(8) Van der Biest, O. O.; Vandeperre, L. *J. Annu. Rev. Mater. Sci.* **1999**, *29*, 327.
(9) Corni, I.; Ryan, M.; Boccaccini, A. *J. Eur. Ceram. Soc.* **2008**, *28*, 1353.
(10) Gani, M. S. *J. Ind. Ceram. Electrophoretic Deposition: A Review* **1994**, *14*, 163.
(11) Besra, L.; Liu, M. *Prog. Mater. Sci.* **2007**, *52*, 1.
(12) Boccaccini, A. R.; Cho, J.; Roether, J. A. C.; Thomas, B. J.; Minay, E. J.; Shaffer, M. S. P. *Carbon* **2006**, *44*, 3149.
(13) Cao, G. Z. *J. Phys. Chem. B* **2004**, *108*, 19921.
(14) Giersig, M.; Mulvaney, P. *Langmuir* **1993**, *9*, 3408.
(15) Teranishi, T.; Hosoe, M.; Tanaka, T.; Miyake, M. *J. Phys. Chem. B* **1999**, *103*, 3818.
(16) Bailey, R. C.; Stevenson, K. J.; Hupp, J. T. *Adv. Mater.* **2000**, *12*, 1930.
(17) Fang, J.; Yi, Y.; Ding, B.; Song, X. *Appl. Phys. Lett.* **2008**, *92*, 131115.
(18) (a) Prochazka, M.; Mojzes, P.; Stepaned, J.; Vlckova, B.; Turpin, P. Y. *Anal. Chem.* **1997**, *69*, 5103. (b) Yang, S. K.; Cai, W. P.; Zeng, H. B.; Li, Z. G. *J. Appl. Phys.* **2008**, *104*, 023516.
(19) *Optical Properties of Metal Clusters*; Kreibig, U., Vollmer, M., Eds.; Springer: Berlin, Germany, 1995.
(20) Fojtik, A.; Henglein, A. *Phys. Chem.* **1993**, *97*, 252.
(21) Yeh, M. S.; Yang, Y. S.; Lee, Y. P.; Lee, H. F.; Yeh, Y. H.; Yeh, C. S. *J. Phys. Chem. B* **1999**, *103*, 6581.
(22) Mafune, F.; Kohno, J.; Takeda, Y.; Kondow, T. *J. Phys. Chem. B* **2002**, *106*, 8555. J. Phys. Chem. B. 2003, *107*, 4218;
(23) Patil, P.; Phase, D. M.; Kulkarni, S. A.; Ghaisas, S. V.; Kulkarni, S. K.; Kanetkar, S. M.; Ogale, S. B.; Bhide, V. G. *Phys. Rev. Lett.* **1987**, *58*, 238.
(24) Korgel, B. A.; Fitzmaurice, D. *Adv. Mater.* **1998**, *10*, 661.
(25) Tang, Z.; Kotov, N. A.; Ciersig, M. *Science* **2002**, *297*, 237.
(26) Cho, K. S.; Talapin, D. C.; Gaschler, W.; Murray, C. B. *J. Am. Chem. Soc.* **2005**, *127*, 7140.
(27) Pradhan, N.; Xu, H.; Peng, X. *Nano Lett.* **2006**, *6*, 720.
(28) Ethayaraja, M.; Bandyopadhyaya, R. *Langumir* **2007**, *23*, 6418.
(29) Zeng, H. B.; Liu, P. S.; Cai, W. P.; Cao, X. L.; Yang, S. K. *Cryst. Growth Des.* **2007**, *7*, 1092.
(30) Note: 5 mL of trisodium citrate aqueous solution (50 mg in 20 mL of water) was added, dropwise, to a heated (95 °C) solution of $AgNO_3$ (66 mg in 100 mL of water) while stirring. The mixture was kept at 95 °C for 15 min, and then cooled to room temperature. Lee, P.; Meisal, D. *J. Phys. Chem.* **1982**, *86*, 3391.

JP901961H